Hindawi
Mobile Information Systems
Volume 2020, Article ID 9049284, 8 pages
https://doi.org/10.1155/2020/9049284

Research Article

Analysis and Design of Systematic Rateless Codes in FH/BFSK System with Interference

Jingke Dai, Peng Zhao, Xiao Chen, and Fenggan Zhang

School of Military Operational Support, Rocket Force University of Engineering, Xi'an 710025, China

Correspondence should be addressed to Jingke Dai; djk029@163.com

Received 19 October 2019; Revised 25 December 2019; Accepted 31 December 2019; Published 10 February 2020

Academic Editor: Ramon Aguero

Copyright © 2020 Jingke Dai et al. This is an open access article distributed under the Creative Commons Attribution License, which permits unrestricted use, distribution, and reproduction in any medium, provided the original work is properly cited.

The asymptotic analysis of systematic rateless codes in frequency hopping (FH) systems with interference is first provided using discretized density evolution (DDE) and compared with the traditional fixed-rate scheme. A simplified analysis with Gaussian assumption of initial message is proposed in the worst case of interference, which has much lower complexity and provides a very close result to DDE. Based on this simplified analysis, the linear programming is employed to design rateless codes and the simulation results on partial-band interference channels show that the optimized codes have more powerful antijamming performance than the codes originally designed for conventional systems.

1. Introduction

Frequency hopping (FH) systems have been extensively employed to combat interference in commercial and military communications [1]. To further enhance the antijamming capability, error-correction codes have also been widely used in FH systems, like convolutional codes [2], Reed–Solomon codes [3], Turbo codes [4, 5], and low-density parity-check (LDPC) codes [6, 7] and all of them are rate-fixed. Since the interference on channels may change randomly and dramatically from time to time, the required code rate or signal power must be adjusted accordingly for uninterrupted communications. Hence, rateless codes, which can automatically adapt their practical rates according to channel conditions, are considered as an alternative scheme for FH systems with interference.

The first practical realization of rateless codes are Luby transform (LT) codes [8], the extension of which are Raptor codes with lower complexity [9]. They are originally designed for binary erasure channels (BEC) but also implemented on noisy channels [10]. The systematic versions of rateless codes have received extensive attention because of their efficient encoding. Systematic LT (SLT) codes and systematic Raptor (SR) codes on BEC are proposed in [9, 11], respectively. Normally, on noisy channels, SLT codes are generated in a direct way [12], i.e., the original information symbols are first transmitted followed by LT-coded symbols. If an inner SLT code is serially concatenated with an outer high-rate LDPC code, the resulting code can also be referred as the SR code [13]. Kite codes are a special class of prefix rateless LDPC codes [14], and they are combined with the multilevel coding scheme to improve transmission reliability [15]. Online fountain codes are proposed in [16], where an optimal encoding strategy is found efficiently based on the instantaneous decoding state. A modified online fountain encoding scheme is introduced in [17] to provide unequal error protection, and a theoretical framework is proposed in [18] to analyze online fountain codes more accurately.

The rateless codes have been applied to FH systems in existing works. The performance of Raptor coded FH systems is investigated under partial-band interference (PBI) and full-band interference (FBI, the case of PBI with interference bandwidth fraction $\rho = 1$) in [19, 20]. The LT-coded differential frequency hopping system with PBI is discussed in [21]. All the results in above works are obtained by computer simulations, i.e., the asymptotic performance is not given. Also, those systems just use the classic codes with degree distributions originally designed for BEC, i.e., they

have not been optimized for FH systems with interference. The authors of [22] use a probability-transfer method to decrease the Raptor codes' average degree weight, but it needs many attempts and the resulting code may not have good performance.

The asymptotic performance of rateless codes is usually studied by discretized density evolution (DDE) [13, 23] and Gaussian approximation (GA) methods [24–26]. As well known, the former provides accurate results but needs much higher computational complexity, whereas the latter uses a one-dimensional (1-D) analysis for faster calculation without much sacrifice in accuracy. However, most existing works focus on the coherent binary phase shift keying (BPSK) system on additive white Gaussian noise (AWGN) channels where the initial message of the log-likelihood ratio (LLR) is symmetrically Gaussian distributed [25], indicating that the GA methods may work very well. In the FH system, binary frequency shift keying (BFSK) and noncoherent (NC) demodulation are more employed, which means that the initial LLR is no longer Gaussian distributed, especially for consideration of interference on channels. Hence, DDE is a better choice to obtain the asymptotic performance of the rateless code in the FH/BFSK system with interference. Furthermore, DDE has been successfully combined with the differential evolution (DE) algorithm to design LDPC codes [7] and SR codes [13], but it is a nonlinear optimization method which costs much computation and spends a long search time.

In this paper, we investigate the asymptotic performance and distribution optimization of systematic rateless codes in FH/BFSK systems with PBI. The main contributions are summarized as follows. Firstly, the asymptotic bit-error-rate (BER) performance and decoding thresholds of SLT codes and SR codes are achieved using DDE and the advantages of rateless codes over fixed-rate codes in the FH system are analyzed extensively. Secondly, since the DDE-DE method is so complicated, we propose a properly simplified method, which assumes the initial LLR of the FH/BFSK system as Gaussian distributed in the worst case of interference. With this GA-LLR, the 1-D analysis based on the extrinsic information transfer (EXIT) chart is employed to analyze the asymptotic performance which is very close to the results provided by DDE. Thirdly, the linear programming (LP) algorithm [25], which is a linear optimization method and then much faster than DE, is combined with the former 1-D analysis to design rateless codes on FBI, i.e., PBI with $\rho = 1$. Both the asymptotic analysis and simulation results show that the optimized codes provide more powerful antijamming capability than the existing codes in the range of $0 < \rho \leq 1$.

2. System Model

The FH communication system model is depicted in Figure 1. The original information sequence $\mathbf{s} = \{s_1, s_2, ..., s_K\}$ is precoded using a high-rate LDPC code to produce the intermediate sequence $\mathbf{e} = \{e_1, e_2, ..., e_{K'}\}$, where the outer code rate is $R_o = K/K'$. The intermediate sequence is further SLT

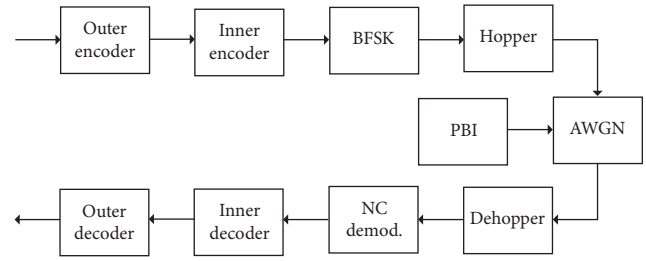

Figure 1: Rateless coded FH/BFSK system model.

encoded to obtain the symbols of Raptor codes, denoted as $\mathbf{c} = \{c_1, c_2, ..., c_N\}$, where the inner code rate is $R_i = K'/N$. Omitting the subscript, the coded symbol $c \in \{0, 1\}$ is modulated to the BFSK symbol with energy $E_s = E_b \cdot R$, where E_b is the bit energy and $R = R_i R_o$ is the overall rate of SR codes. The modulated symbol is transmitted over a frequency slot determined by the hopping pattern, and we only consider the case of one symbol per hop in this paper.

The transmitted signal experiences full-band AWGN as well as the partial-band interference, which is modelled as an on-off jammer and evenly distributes its power over a fraction $\rho \in (0, 1]$ of the frequency range. We set the single-side power spectrum density (PSD) of noise and interference is N_0 and N_j/ρ, respectively. As a result, there are essentially two states on this channel: jammed and unjammed, which are denoted as $J = 1$ and $J = 0$, respectively. At the receiver, the signal is assumed to be perfectly dehopped and the two branches' outputs of the noncoherent (square-law) demodulator is denoted as $\{y_1, y_0\}$.

Without loss of generality, we assume the transmitted symbol $c = 1$ in the current hop and then the conditional PDFs of $\{y_1, y_0\}$ are given by [7]:

$$\begin{cases} p(y_1 \mid c = 1) = \dfrac{1}{N_l} \exp\left(-\dfrac{y_1 + E_s}{N_l}\right) I_0\left(\dfrac{2\sqrt{y_1 E_s}}{N_l}\right), & y_1 > 0, \\ p(y_0 \mid c = 1) = \dfrac{1}{N_l} \exp\left(-\dfrac{y_0}{N_l}\right), & y_0 > 0, \end{cases} \tag{1}$$

where $N_l = N_0 + J(N_j/\rho)$ is determined by the channel state and $I_0(x)$ is the modified zero-order Bessel function of the first kind. Assuming each hop is independent of each other and the channel side information is known, we have the optimal log-likelihood ratio calculated as in [6]:

$$z = \log \frac{P(c = 1 \mid y_1, y_0)}{P(c = 0 \mid y_1, y_0)} = \log \frac{I_0\left(2\sqrt{y_1 E_s}/N_l\right)}{I_0\left(2\sqrt{y_0 E_s}/N_l\right)}. \tag{2}$$

The decoding of inner SLT codes is followed by decoding of outer LDPC codes. The SPA is implemented in the inner decoder according to the related bipartite graph, which is constructed using intermediate symbols and output symbols as variable nodes (VNs) and check nodes (CNs). The message update rules between VNs and CNs are given by [25].

$$u_{m,n}^{(l)} = 2\tanh^{-1}\left[\tanh\left(z_{K'+n}/2\right)\prod_{k\in\{S_n\}\backslash m}\tanh\left(v_{n,k}^{(l)}/2\right)\right], \quad (3)$$

$$v_{n,m}^{(l+1)} = z_m + \sum_{k\in\{S_m\}\backslash n} u_{m,k}^{(l)}, \quad (4)$$

where $u_{m,n}^{(l)}$ and $v_{n,m}^{(l)}$ denote the message passed from the n-th check node to the m-th variable node and the message passed in the opposite direction at the l-th decoding iteration and $\{S_n\}\backslash m$ represents the set of all neighbours of the n-th node except for the m-th node. After the maximum iteration $l_{\max}$, the decision message $v_m^{(l_{\max})} = z_m + \sum_{k\in\{S_m\}} u_{m,k}^{(l_{\max}-1)}$ is provided as the initial LLR to decode outer LDPC codes.

3. Asymptotic Analysis

3.1. Initial LLR on PBI Channels. From (1) and (2), we know that it is hard to get close-form density expression of the initial LLR message due to Bessel functions, unlike the case of the coherent BPSK system. Thus, we use the probability mass function (PMF) instead [13]. Firstly, the continuous variables $\{y_1, y_0\}$ is quantized to $\{\hat{y}_1, \hat{y}_0\}$ with a quantization interval Δ_1. Secondly, calculate the quantized initial message by a two-input function expressed as

$$\begin{aligned}\hat{z} &= F(\hat{y}_1, \hat{y}_0)\\ &= \mathfrak{F}\left(\log\left(I_0\left(2\sqrt{\hat{y}_1 E_s}/N_l\right)/I_0\left(2\sqrt{\hat{y}_0 E_s}/N_l\right)\right)\right),\end{aligned} \quad (5)$$

where $\mathfrak{F}$ is the "quantization operator" ensuring that $\hat{z}$ takes values in a discrete set $\{z_{\min}, z_{\min}+\Delta_2, z_{\min}+2\Delta_2, \ldots, z_{\min}+k\Delta_2, \ldots, z_{\max}\}$ with a quantization interval Δ_2. Finally, calculate the probability of $\hat{z} = z_{\min} + k\Delta_2$ as given by

$$p_{\hat{z}_k} = \sum_{(i,j):\, k\Delta = F(i\Delta, j\Delta)} p_{\hat{y}_1}[i]\, p_{\hat{y}_0}[j], \quad (6)$$

where the probability masses $p_{\hat{y}_1}[i]$ and $p_{\hat{y}_0}[j]$ are the quantized results from equation (1). Finally, the assemble of $p_{\hat{z}_k}$ gives the PMF of $\hat{z}$. Note that N_l in (5) has two possible values, thus $p_{\hat{z}_k}$ also has two possible values which gives the PMF of $\hat{z}$ denoted as $p_{z,J}$ and $p_{z,NJ}$ corresponding to jammed and unjammed states, respectively. The unconditional PMF of $\hat{z}$ is written as

$$p_z = \rho p_{z,J} + (1-\rho) p_{z,NJ}. \quad (7)$$

Setting $\Delta_1 = 0.01$, $\Delta_2 = 0.05$, $z_{\min} = -20$, and $z_{\max} = 40$, the PMF of initial LLR under the channel with symbol signal-to-noise ratio (SNR) $E_s/N_0 = 10$ dB, symbol signal-to-jamming ratio (SJR) $E_s/N_j = 5$ dB, and $\rho = 0.7$ is depicted in Figure 2. It is seen that the PMF has two peaks caused by different channel states and is no longer Gaussian distributed, which implies that the Gaussian approximation-based method may not be employed to investigate the asymptotic performance of rateless codes on PBI channels (for $\rho < 1$, at least). Hence, we consider the DDE which does not require Gaussian initial LLR.

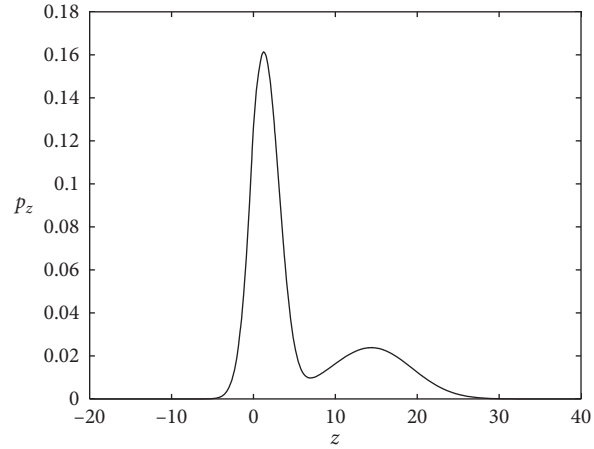

Figure 2: PMF of initial LLR in the FH/BFSK system with $E_s/N_0 = 10$ dB, $E_s/N_j = 5$ dB, and $\rho = 0.7$.

3.2. Asymptotic Performance of SLT and SR Codes. We define the generation matrix of inner SLT codes as $\mathbf{G}_{\mathrm{SLT}} = [\mathbf{I}_{K'}\mathbf{G}_{\mathrm{LT}}]$, where $\mathbf{I}_{K'}$ is an identity matrix having a size of $K' \times K'$ and $\mathbf{G}_{\mathrm{LT}}$ of size $K' \times (N - K')$ is the generation matrix of the conventional LT code [25]. The overhead of the inner SLT code is defined by $\varepsilon = (N - K')/K'$ which is related with the code rates as $\varepsilon = 1/R_i - 1 = R_o/R - 1$.

The degree distributions related with the bipartite graph corresponding to $\mathbf{G}_{\mathrm{LT}}$ is defined as follows. Using polynomial notations, the check node degree distributions is written compactly as $\Omega(x) = \sum_{j=1}^{d_c}\Omega_j x^j$, where d_c is the maximum degree. The corresponding edge degree distribution is calculated by $\omega(x) = \sum_{j=1}^{d_c}\omega_j x^{j-1} = \Omega'(x)/\Omega'(1)$ and the average degree of CNs is given by $\beta = \Omega'(1)$. The average degree of VNs is denoted by α, and then the variable nodes and edge degrees are both assumed to be Poisson distributed as $\Lambda(x) = e^{\alpha(x-1)}$ and $\lambda(x) = e^{\alpha(x-1)}$, respectively [25]. However, the power series can also be truncated to obtain polynomials that is very close to the exponential, i.e., $\Lambda(x) = \sum_{i=1}^{d_v}\Lambda_i(\alpha)x^i$ and $\lambda(x) = \sum_{i=1}^{d_v}\lambda_i(\alpha)x^{i-1}$, where d_v is large enough to ensure $\Lambda(1) \approx 1$.

We denote the PMF of the message passed from CNs and VNs by p_u and p_v, respectively. The updating rules of CNs and VNs are summarized as follows:

$$\begin{aligned}p_u &= \sum_{j=1}^{d_c}\omega_j\,\mathfrak{R}\left(p_z, \mathfrak{R}\left(p_v, \mathfrak{R}\left(p_v, \ldots, \mathfrak{R}\right)\right)\right)\\ &= \sum_{j=1}^{d_c}\omega_j\mathfrak{R}\left(p_z, \mathfrak{R}^{j-1}p_v\right),\end{aligned} \quad (8)$$

$$p_v = \sum_{i=1}^{d_v}\lambda_i\left[p_z \otimes \left(\overset{i-1}{\otimes}\, p_u\right)\right], \quad (9)$$

where $\mathfrak{R}$ is a two-input operator defined in [23] to calculate the PMF of quantized message emanating from check nodes and $\otimes$ denotes convolution calculation. The DDE of outer LDPC codes is similar to the above rules, only that the channel message PMF p_z is removed at the CNs. The detail of DDE on

the SR code is referred to [13], and here we just need to replace the initial LLR of the BPSK system by equation (7).

The asymptotic BER performance of SLT codes and SR codes obtained by DDE under different PBI bandwidth fraction ρ is shown in Figure 3, where SNR is fixed to 10 dB and the outer code is fixed to a 0.98-rate regular (4, 200)-LDPC code. The degree distribution of the inner code is fixed to the optimized rate 1/2 results in [13], which is rewritten as

$$\Omega_1(x) = 0.00477x + 0.26101x^2 + 0.09240x^3 + 0.06913x^8 + 0.51223x^9 + 0.06046x^{60}. \tag{10}$$

In Figure 3(a), the overall code rate is fixed to 1/2 and SJR is variable, whereas in Figure 3(b), SJR is fixed to 5 dB and the overhead of the inner code ε (then the code rate R) is variable. In the range of small SJR or overhead, the performance of SLT codes and SR codes is very close to each other, indicating that the outer code cannot correct residual errors from the inner code. The BER of the SLT code decreases as either SJR or overhead increases but high error floors are observed.

Once the BER of the inner SLT code achieves a critical BER, which is firstly introduced in [23], the BER of the SR code decreases very sharply. It is easy to calculate the critical BER using DDE [23], which is equal to 0.0039 for the 0.98-rate regular LDPC code. In addition, the case of $\rho = 1$ has the worst performance, where PBI has actually become the full-band interference.

3.3. Comparison of Rateless Codes and Fixed-Rate Codes. To compare the rateless codes and conventional fixed-rate codes in the FH system, their decoding thresholds are investigated under different PBI bandwidth fractions ρ. From Figure 3(b), we know the BERs of SR codes tend to zero as the inner BER achieves critical BER and the corresponding overhead can be referred as the decoding threshold. According to the relation between overhead and code rate presented in Section 2, we plot the rate thresholds of SR codes for different ρ with various E_s/N_j in Figure 4. The classic 1/2-rate regular (3, 6) LDPC is taken as the fixed-rate code for comparison, and the SJR-decoding thresholds associated with the right axis are also depicted in Figure 4.

It is seen that the SJR-threshold of the LDPC code grows as ρ increases and the worst case appears at $\rho = 1$ corresponding to the threshold of 5.71 dB. As ρ may change randomly over time, the SJR of the fixed-rate coded FH system must be set to be larger than the threshold of the worst case, which in essence is a waste of power or rate for the cases of $\rho < 1$. However, Raptor codes can "automatically" choose the proper rates for different ρ, e.g., under the SJR of 5.71 dB, the rate thresholds of Raptor codes are 0.74 and 0.51 for $\rho = 0.1$ and $\rho = 1$, respectively. Meanwhile, the Raptor code is more adaptable to environment with dramatic SJR changes. When SJR decreases, e.g., to 4 dB, the Raptor can still work as long as we continue to send coded symbols (decreasing actual rate) but the specific fixed-rate code cannot. When SJR increases, e.g., to 7 dB, the Raptor code can work with a higher rate than the 1/2-rate LDPC code. In general, rateless codes are more flexible and more robust than the fixed-rate codes on PBI channels.

4. Simplified Analysis under FBI

4.1. Gaussian Assumption of Initial LLR. Although the asymptotic BER and decoding thresholds have been obtained by DDE, the employed degree distribution is originally designed for the coherent BPSK system, which means that stronger antijamming capability may be achieved if we can optimize the degree distribution for the noncoherent FH system. The conventional method combined with DDE is differential evolution, but it has a pretty high complexity and long search time. The linear programming method can also be used to design Raptor/LT codes, and it is much simpler and faster than DE. But the LP method is usually combined with the one-dimensional analysis method, e.g., EXIT chart, which requires the initial LLR being Gaussian distributed.

From Figure 2, we know that LLR on the PBI channel is not Gaussian but we find that the PMF of initial LLR in the FH/BFSK system can be approximated by a symmetric Gaussian density when $\rho = 1$, which happened to be the worst case of interference. Using (7), we have $p_z = p_{z,J}$ at this time and the mean of z, denoted by m_z, can be easily calculated based on p_z. We approximate p_z by a Gaussian density with mean m_z and variance $2m_z$ and plot the actual PMF as well as the approximated density shown in Figure 5. The curves in one pair are very close to each other, which indicate that the one-dimensional analysis could be employed to investigate asymptotic performance and be further combined with LP to design codes.

4.2. One-Dimensional Analysis. Since the initial LLR is approximately Gaussian distributed when $\rho = 1$, the EXIT chart can be implemented to analyze the asymptotic performance of the inner SLT codes. Assuming the all-zero codeword is transmitted, the mutual information of z is computed by [24] as follows:

$$J(\sigma) = 1 - \frac{1}{\sqrt{2\pi}\sigma}\int_{-\infty}^{\infty}\exp\left[-\frac{\left(\xi - \sigma^2/2\right)^2}{2\sigma^2}\right]\log_2\left(1 + e^{-\xi}\right)d\xi, \tag{11}$$

where $J(\sigma)$ is a monotonically increasing function and has an inverse function $\sigma = J^{-1}(I)$. Both $J(\cdot)$ and $J^{-1}(\cdot)$ do not have close-form expressions, but they can be closely approximated as suggested in [27].

From (4) we can calculate the mutual information of VNs at the l-th iteration as

$$I_{E,V}^{(l)}\left[I_{E,C}^{(l-1)}\right] = \sum_{i=1}^{d_v}\lambda_i(\alpha)J\left(\sqrt{\sigma_{\text{ch1}}^2 + (i-1)\sigma_V^2}\right), \tag{12}$$

where $\sigma_{\text{ch1}}^2 = 2m_z$ is the variance of initial LLR and $\sigma_V^2 = \left\{J^{-1}\left[I_{E,C}^{(l-1)}\right]\right\}^2$ is the message variance of CNs in the previous iteration. The mutual information outputted by CNs at the l-th iteration is given by [24] as follows:

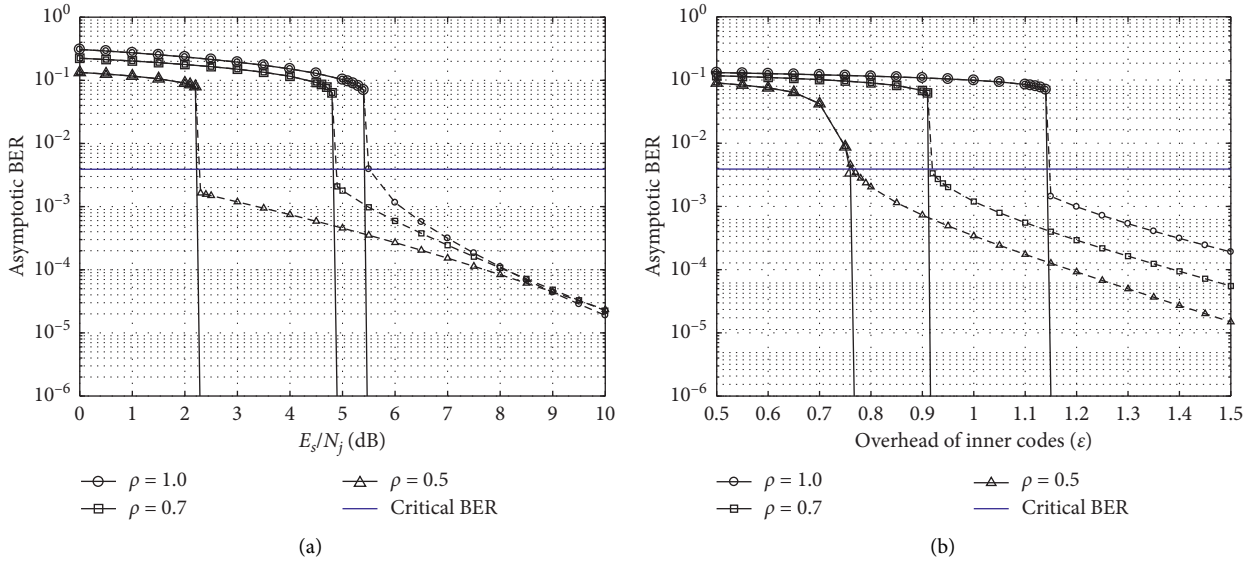

Figure 3: Asymptotic BER of SLT codes and SR codes with $E_s/N_0 = 10$ dB. The dotted lines are BERs obtained after inner decoding and the solid lines are those after outer decoding. (a) $R = 1/2$. (b) $E_s/N_j = 5$ dB.

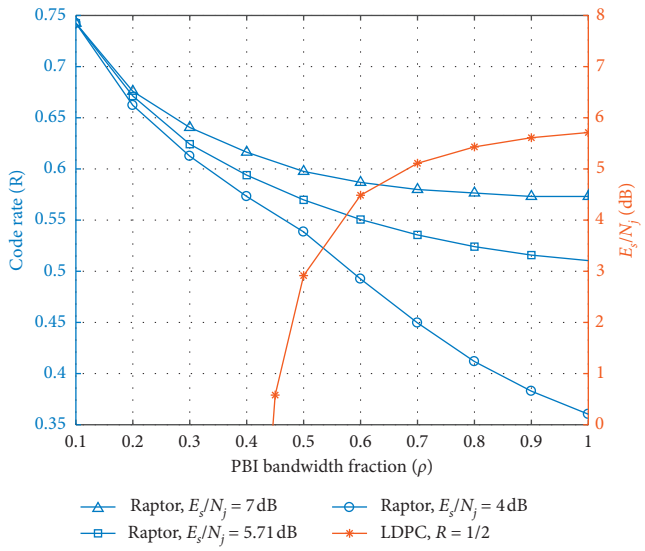

Figure 4: Rate thresholds of Raptor codes and SJR-thresholds of LDPC codes for different ρ.

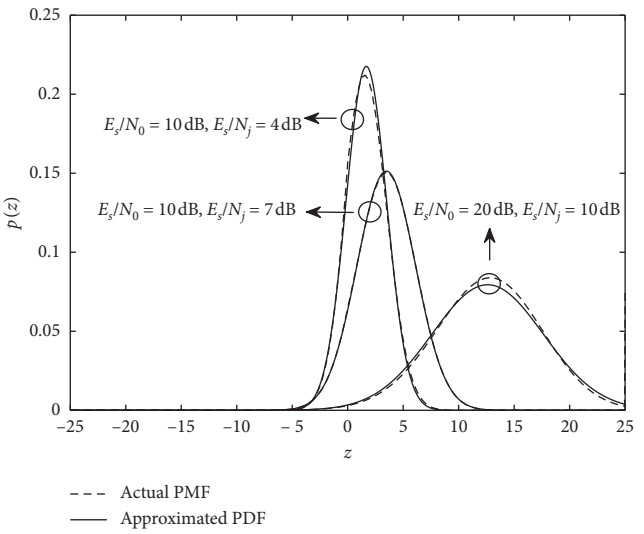

Figure 5: Actual PMF of initial LLR and their Gaussian approximated PDF under $\rho = 1$.

$$I_{E,C}^{(l)}\left(I_{E,V}^{(l)}\right) = \sum_{j=1}^{d_c} \omega_j \left[1 - J\left(\sqrt{\sigma_{\text{ch2}}^2 + (j-1)\sigma_C^2}\right)\right], \quad (13)$$

where $\sigma_{\text{ch2}} = J^{-1}[1 - J(\sqrt{2m_z})]$ and $\sigma_C = J^{-1}[1 - I_{E,V}^{(l)}]$. Combining (12) and (13), we can get the iteration expression of $I_{E,C}^{(l)}$ as the function of $I_{E,C}^{(l-1)}$, σ, and α as given by

$$I_{E,C}^{(l)} = T\left(I_{E,C}^{(l-1)}, \sigma, \alpha\right) = \sum_{j=1}^{d_c} \omega_j \left[1 - J\left(\sqrt{\sigma_{\text{ch2}}^2 + (j-1)\left(J^{-1}\left(1 - I_{E,V}^{(l)}\left(I_{E,C}^{(l-1)}\right)\right)\right)^2}\right)\right]. \quad (14)$$

At the end of iteration $l_{\max}$, the inner decoder outputs the extrinsic information provided to the outer decoder as given by

$$I_{\text{ext}} = \sum_{i=1}^{d_v} \Lambda_i J\left(\sqrt{4/\sigma^2 + i\left(J^{-1}\left(I_{E,C}^{(l_{\max})}\right)\right)^2}\right), \quad (15)$$

and the corresponding error probability is calculated as

$$P_e^{\text{SLT}} = \sum_{i=1}^{d_v} \Lambda_i(\alpha) Q\left[\sqrt{1/\sigma^2 + i\left(J^{-1}\left(I_{E,C}^{(l_{\max})}\right)\right)^2}/4\right], \quad (16)$$

where the function $Q(x) = 1/\sqrt{2\pi}\int_x^{+\infty} e^{-t^2/2}dt$.

Using the above method and setting $E_s/N_0 = 10$ dB and $E_s/N_j = 4$ dB, we depict the asymptotic BERs of the inner

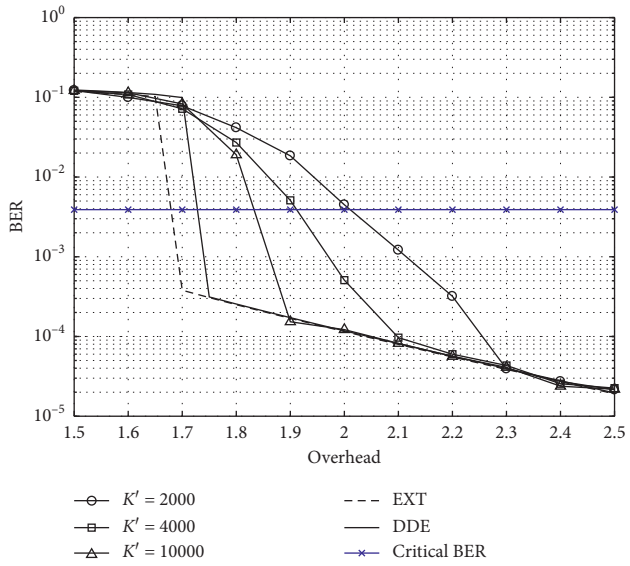

Figure 6: The comparison of asymptotic performance and simulation results of SLT codes.

SLT code of $\Omega_1(x)$ in Figure 6, which is represented by "EXIT". Also shown are those achieved by DDE and the simulated BERs of SLT codes with finite length K' equal to 2000, 4000, and 10000, respectively. We observe that the EXIT curve is very close to the DDE curve and both of them can be taken as the asymptotic performance of simulation results, indicating that the proposed Gaussian assumption of initial LLR under $\rho = 1$ is very effective. In Figure 6, the critical BER of the outer codes is also presented, and its intersection points with asymptotic curves correspond to the decoding thresholds of Raptor codes. It is seen that the threshold of EXIT is lower than DDE which is opposite in the ordinary BPSK system [13]. This is because the initial LLR of the FH/BFSK system is assumed to be Gaussian, which is different from the real situation (see Figure 5), but the initial LLR of the ordinary BPSK system is really Gaussian and the gap between EXIT and DDE is caused by Gaussian assumption of the message from CNs. Though the asymptotic performance by EXIT is slightly different from that by DDE, it can still be employed to design codes with good performance.

5. Code Design and Simulation Results

Technically, the optimal distributions of inner SLT codes are different for different ρ, but it is unrealistic for practical communications to switch distributions in real time according to the current channel conditions. Hence, the optimized distributions for the worst case of interference, naturally, are a good choice for all situations. Besides, we are lucky that the worst case of interference occurs at $\rho = 1$ so that the PMF of initial LLR can be approximated by a Gaussian density and the EXIT analysis can be combined with the standard LP method, which is described by the following model:

$$\begin{aligned} \min: \quad & \sum_{i=1}^{d_c} \frac{\omega_j}{j}, \\ \text{s.t.} \quad & TI_{E,C}^{l-1}, \sigma, \alpha > I_{E,C}^{l-1}, I_{E,C}^{l-1} \in \left[0, I_{E,C}^{\max}\right], \\ & l = 1, 2, \ldots, L, \\ & \sum_{i=1}^{d_c} \omega_j = 1, \\ & \omega_j \geq 0, \quad j = 1, \ldots, d_c. \end{aligned} \tag{17}$$

In the optimization model, the design objective is to minimize the overhead $\varepsilon = \alpha/\beta = \alpha \sum_{j=1}^{d_c} \omega_j / j$. The second and third constraints ensure the distributions validity. According to (14), the first constraint ensures that the tracking variable converges to a fixed value $I_{E,C}^{\max}$ in iterations.

We fix the SNR as 10 dB and set the critical BER as 0.0039 and search the good distributions of SLT codes using LP under different SJR. The resulting degree distributions and corresponding overhead thresholds are listed in Table 1, in which ε_E denotes the required overhead of inner codes achieving critical BER by the EXIT method and ε_D denotes the required overhead by the DDE method. We can see that the overhead thresholds obtained by two methods are very close to each other, confirming that the optimized codes indeed have good performance. Specifically, $\varepsilon_E = \varepsilon_D$ for SJR = 6 dB and SJR = 7 dB is not a surprising result since the approximated initial LLR is almost the same with the real one (see Figure 5).

It is noted that all the optimized distributions are obtained with condition $\rho = 1$. To investigate the performance of optimized distributions under $\rho < 1$, we use DDE to get the overhead thresholds of optimized codes and code with $\Omega_1(x)$ under SJR = 4 dB and SJR = 7 dB which are compared in Figure 7. When SJR = 7 dB, the optimized code has smaller thresholds than $\Omega_1(x)$ for all ρ. At the point of $\rho = 1$, the overhead thresholds of two codes are 0.53 and 0.71, respectively. If the outer code rate is fixed to 0.98, the corresponding overall rate of the optimized code increases about 11.7% compared to the code with $\Omega_1(x)$. When SJR = 4 dB, the optimized code also has better performance than the code with $\Omega_1(x)$ for large ρ but they are very close when ρ is small. Considering that the PBI mainly works on the range of large ρ, we say that our optimized codes have more powerful anti-jamming capacity than the traditional code.

We apply the optimized degree distribution to the codes with information length $K = 4000$ under serious interference (SJR = 4 dB). The outer code is set as the 0.98-rate regular LDPC code, and SNR is fixed to 10 dB. The simulated BERs of Raptor codes in the FH/BFSK system with $\rho = 0.7$ and $\rho = 1$ are plotted in Figure 8. As shown in this figure, the optimized code provides better performance than the existing code for both PBI and FBI conditions, verifying the effectiveness of our design method.

Table 1: The optimized degree distributions of inner SLT codes with SNR = 10 dB.

SJR	4 dB		5 dB		6 dB		7 dB	
	$\Omega_{\text{opt1}}(x)$	$\alpha = 13.5$	$\Omega_{\text{opt2}}(x)$	$\alpha = 11$	$\Omega_{\text{opt3}}(x)$	$\alpha = 9$	$\Omega_{\text{opt4}}(x)$	$\alpha = 8$
	Ω_5	0.59654	Ω_6	0.53805	Ω_7	0.29357	Ω_9	0.33414
	Ω_6	0.28390	Ω_7	0.36372	Ω_8	0.61311	Ω_{10}	0.58986
	Ω_{30}	0.09375	Ω_{44}	0.07748	Ω_{59}	0.06836	Ω_{83}	0.01170
	Ω_{87}	0.01826	Ω_{88}	0.00901	Ω_{60}	0.02496	Ω_{84}	0.06430
	Ω_{88}	0.00755	Ω_{89}	0.01174				
ε_E	1.39		1.00		0.73		0.53	
ε_D	1.43		1.03		0.73		0.53	

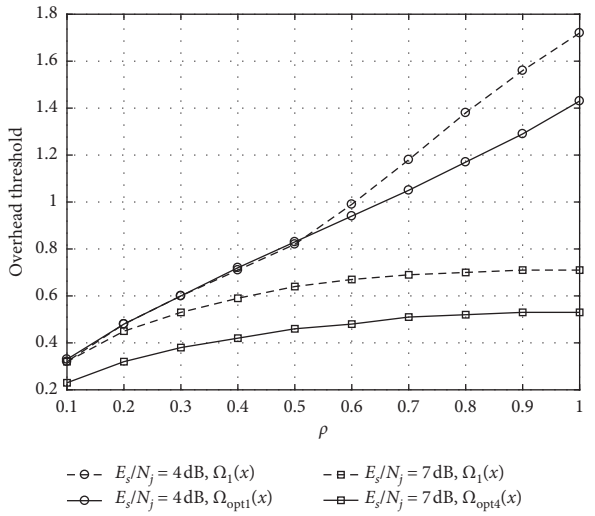

Figure 7: Overhead thresholds of inner SLT codes for different ρ.

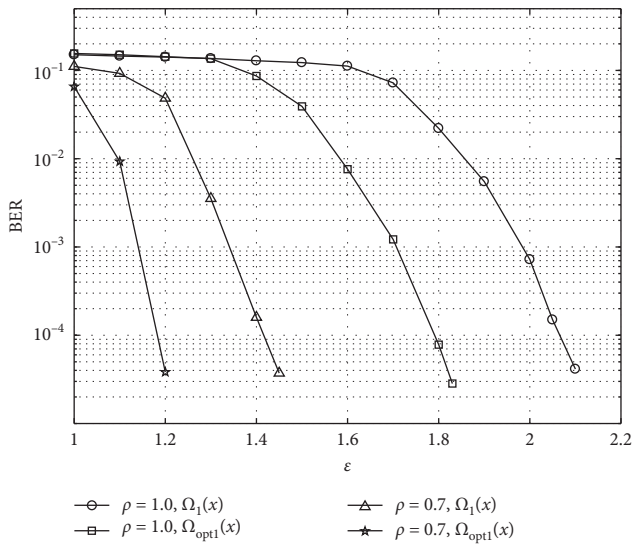

Figure 8: Simulated BER of SR codes versus overhead under SJR = 4 dB and SNR = 10 dB.

6. Conclusions

The asymptotic performance of systematic rateless codes in the FH/BFSK system with PBI has been obtained and compared with the fixed-rate LDPC codes. The rateless codes are more flexible and more robust than fixed-rate codes on PBI channels. The worst case of interference for the rateless-coded FH/BFSK system usually appears at the point of $\rho = 1$ where PBI become to FBI. Under FBI, the initial LLR is assumed to be Gaussian distributed and then the 1-D analysis based on the EXIT chart is employed to investigate the asymptotic performance which is very close to the result by DDE. The code degree distributions are designed using linear programming which is combined with the 1-D analysis. On PBI channels, the optimized codes in the FH/BFSK system provide outstanding antijamming performance compared with the code originally designed for the conventional BPSK system. In addition, the coding scheme of the FH system in this paper concentrates on the SR codes and some novel rateless codes, such as Kite codes and online fountain codes, will be considered in our future works.

Data Availability

The numerical and simulation data used to support the findings of this study are included within the supplementary information file.

Conflicts of Interest

The authors declare that there are no conflicts of interest regarding the publication of this paper.

Acknowledgments

This work was supported by the National Natural Science Foundation of China (Grant no. 61501469) and the China Postdoctoral Science Foundation (Grant no. 2015M572782).

References

[1] C. Kim, J. S. No, J. Park et al., "Anti-jamming partially regular LDPC codes for follower jamming with Rayleigh block fading in frequency hopping spread spectrum," in *Proceedings of the International Conference on Information & Communication Technology Convergence*, pp. 583–587, Jeju, South Korea, October 2016.

[2] J. S. Lee, R. H. French, and L. E. Miller, "Error-correcting codes and nonlinear diversity combining against worst case partial-band noise jamming of frequency-hopping MFSK systems," *IEEE Transactions on Communications*, vol. 36, no. 4, pp. 471–478, 1988.

[3] M. Pursley and W. Stark, "Performance of reed-solomon coded frequency-hop spread-spectrum communications in

partial-band interference," *IEEE Transactions on Communications*, vol. 33, no. 8, pp. 767–774, 1985.

[4] U.-C. Fiebig and P. Robertson, "Soft-decision and erasure decoding in fast frequency-hopping systems with convolutional, turbo, and Reed-Solomon codes," *IEEE Transactions on Communications*, vol. 47, no. 11, pp. 1646–1654, 1999.

[5] D. Torrieri, S. Cheng, and M. C. Valenti, *Robust Frequency Hopping for Interference and Fading Channels*, in *Proceedings of the IEEE International Conference on Communications*, pp. 1–7, Glasgow, UK, June 2007.

[6] X., C. Wu, X. Zhao, You, and S. Li, "Robust diversity-combing receivers for LDPC coded FFH-SS with partial-band interference," *IEEE Communications Letters*, vol. 11, no. 7, pp. 613–615, 2007.

[7] J. Dai, Y. Jing, and M. Yao, "Analysis of LDPC code in the FH system with partial-band interference," *IET Communications*, vol. 11, no. 17, pp. 2585–2595, 2017.

[8] M. Luby, "LT codes," in *Proceedings of the 43rd Symposium on Foundations of Computer Science, ser. FOCS '02*, pp. 271–280, Washington, DC, USA, 2002.

[9] A. Shokrollahi, "Raptor codes," *IEEE Transactions on Information Theory*, vol. 52, no. 6, pp. 2551–2567, 2006.

[10] B. Sivasubramanian and H. Leib, "Fixed-rate raptor codes over Rician fading channels," *IEEE Transactions On Vehicular Technology*, vol. 57, no. 6, pp. 3905–3911, 2008.

[11] X. Yuan and L. Ping, "On systematic LT codes," *IEEE Communications Letters*, vol. 12, no. 9, pp. 681–683, 2008.

[12] T. D. Nguyen, L. L. Yang, and L. Hanzo, "Systematic Luby transform codes and their soft decoding," in *Proceedings of the IEEE Workshop on Signal Processing Systems*, pp. 67–72, Shanghai, China, October 2007.

[13] A. Kharel and L. Cao, "Asymptotic analysis and optimization design of physical layer systematic rateless codes," in *Proceedings of 15th IEEE Consumer Communications and Networking Conference*, pp. 1–6, Las Vegas, NV, USA, January 2018.

[14] B. Bai, B. Bai, and X. Ma, "Simple rateless error-correcting codes for fading channels," *Science China Information Sciences*, vol. 55, no. 10, pp. 2194–2206, 2012.

[15] D. Jia, C. Shangguan, Z. Fei et al., "Multilevel coding technology based on Kite code in AWGN channel," *Transactions of Beijing Institute of Technology*, vol. 37, no. 4, pp. 360–364, 2017.

[16] Y. Cassuto and A. Shokrollahi, "Online fountain codes with low overhead," *IEEE Transactions on Information Theory*, vol. 61, no. 6, pp. 3137–3149, 2015.

[17] J. Huang, Z. Fei, C. Cao, M. Xiao, and D. Jia, "On-line fountain codes with unequal error protection," *IEEE Communications Letters*, vol. 21, no. 6, pp. 1225–1228, 2017.

[18] J. Huang, Z. Fei, C. Cao, M. Xiao, and D. Jia, "Performance analysis and improvement of online fountain codes," *IEEE Transactions on Communications*, vol. 66, no. 12, pp. 5916–5926, 2018.

[19] F. Gao, X. Zeng, and X. Bu, "Research of anti-interference performance of digital fountain codes in Frequency hopping communications," *Transactions of Beijing Institute of Technology*, vol. 32, no. 4, pp. 420–424, 2012.

[20] X. Bu, P. Li, Y. Wang et al., "Transmission design and performance of a strong anti-jamming frequency hopping system based on fountain codes," *Transactions of Beijing Institute of Technology*, vol. 34, no. 11, pp. 1186–1190, 2014.

[21] W. Zhu, B. Yi, and L. Gan, "Performance research of fountain-DFH concatenated coding systems over AWGN with partial-band noise jamming," *Systems Engineering and Electronics*, vol. 38, no. 3, pp. 665–671, 2016.

[22] F. Gao, X. Zeng, and X. Bu, "Improved scheme for short-length Raptor codes based on frequency hopping communication," *Transactions of Beijing Institute of Technology*, vol. 33, no. 4, pp. 403–407, 2013.

[23] A. Kharel and L. Cao, "Analysis and design of physical layer raptor codes," *IEEE Communications Letters*, vol. 22, no. 3, pp. 450–453, 2018.

[24] I. Hussain, X. Xiao, and L. K. Rasmussen, "Error floor analysis of LT codes over the additive white Gaussian noise channel," in *Proceedings of IEEE Global Telecommunications Conference*, pp. 1–5, Kathmandu, Nepal, 2011.

[25] S. Xu and D. Xu, "Optimization design and asymptotic analysis of systematic Luby transform codes over BIAWGN channels," *IEEE Transactions on Communications*, vol. 64, no. 8, pp. 3160–3168, 2016.

[26] D. Deng, D. Xu, and S. Xu, "Optimisation design of systematic LT codes over AWGN multiple access channel," *IET Communications*, vol. 12, no. 11, pp. 1351–1358, 2018.

[27] S. T. Brink, G. Kramer, and A. Ashikhmin, "Design of low-density parity-check codes for modulation and detection," *IEEE Transactions on Communications*, vol. 52, no. 4, pp. 670–678, 2004.